Fish and Shellfish Immunology 89 (2019) 228–236

Contents lists available at ScienceDirect

Fish and Shellfish Immunology

journal homepage: www.elsevier.com/locate/fsi

Full length article

A new member of the runt domain family from Pacific oyster *Crassostrea gigas* (*Cg*Runx) potentially involved in immune response and larvae hematopoiesis

Xiaorui Song[a], Ying Song[a], Miren Dong[a], Zhaoqun Liu[a], Weilin Wang[a], Lingling Wang[a], Linsheng Song[a,b,*]

[a] *Liaoning Key Laboratory of Marine Animal Immunology, Dalian Ocean University, Dalian, 116023, China*
[b] *Laboratory of Marine Fisheries Science and Food Production Process, Qingdao National Laboratory for Marine Science and Technology, Qingdao, 266071, China*

ARTICLE INFO

Keywords:
Runx transcription factors
Pacific oyster *Crassostrea gigas*
Hematopoiesis
Whole-mount immunofluorescence assay

ABSTRACT

The Runx family is a kind of heteromeric transcription factors, which is defined by the presence of a runt domain. As transcriptional regulator during development and cell fate specification, Runx is best known for its critical roles in hematopoiesis. In the present study, a Runx transcription factor (designed as *Cg*Runx) was identified and characterized from the oyster *Crassostrea gigas*. The complete coding sequence of *Cg*Runx was of 1638 bp encoding a predicted polypeptide of 545 amino acids with one conserved runt domain, which shared high similarity with other reported Runx proteins. *Cg*Runx was highly expressed in hemocytes, gill and mantle both at the protein and nucleic acid levels. *Cg*Runx protein was localized specifically in the cell nuclei of hemocytes, and distributed at the tubule lumen of gill filament. During the larval developmental stages, the mRNA transcripts of *Cg*Runx gradually increased after fertilization, reached to a relative high level at the 8 cell embryos and the blastula stage of 2–4 hpf (hours post fertilization) (about 40-fold), and peaked at early trochophore larvae (10 hpf) (about 60-fold). Whole-mount immunofluorescence assay further revealed that the abundant immunofluorescence signals of *Cg*Runx distributed through the whole embryo at blastula stage (5 hpf), and progressively reduced with the development to a ring structure around the dorsal region in trochophore larvae (10 hpf). Scattered positive immunoreactivity signals finally appeared in the velum region of D-veliger larvae. After LPS and *Vibrio splendidus* stimulations, the expression levels of *CgRunx* mRNA in hemocytes were up-regulated significantly compared with that in the control (0 h), which were 2.98- and 2.46-fold ($p < 0.05$), 2.67- and 1.5-fold ($p < 0.05$), 2.36- and 1.38-fold ($p < 0.05$) at 3 h, 6 h and 12 h, respectively. These results collectively suggested that *Cg*Runx involved in immune response and might participate in larvae hematopoiesis in oyster.

1. Introduction

Runt-related (Runx) proteins form a family of transcription factors that share a highly conserved runt domain of 128 amino acids, which is required for DNA binding and protein-protein interactions [1]. The name Runx is derived from the first member of the Runx family, runt in *Drosophila melanogaster* [2], which was first identified as a pair-rule gene in embryonic patterning, and later it was found to play a role in sex determination and neural development [3,4]. So far, three highly conserved runt domain genes, Runx1, Runx2 and Runx3, have been identified in vertebrates and they share a high degree of functional redundancy in several biological processes, such as hematopoiesis [5,6], neurogenesis [7], and immune response [1]. Of relevance to the present study, Runx1 and Runx3 are best known for the essential roles in hematopoiesis and immunity [1,5].

Runx1 (also known as AML1, Cbfa2, and Pebpa2b) is required for the emergence, formation and/or function of definitive hematopoietic stem cells (HSC) [8]. Histological studies showed that Runx1 was specially expressed throughout all hematopoietic lineages, and it was necessary for the emergence of the first HSC to the terminal differentiation [8,9]. No functional HSCs are found in any of the early hematopoietic sites, i.e., aorta-gonad-mesonephros (AGM) region, yolk sac or fetal liver in E10, E11, and E12. Homozygous mutant Runx1 embryos leaded to a complete lack of definitive hematopoiesis, suggesting that Runx1

---

[*] Corresponding author. Liaoning Key Laboratory of Marine Animal Immunology, Dalian Ocean University, Dalian, 116023, China.
E-mail address: lshsong@dlou.edu.cn (L. Song).

https://doi.org/10.1016/j.fsi.2019.03.066
Received 28 August 2018; Received in revised form 14 March 2019; Accepted 26 March 2019

was required for HSC emergence [10]. Furthermore, homozygous mutation of Runx1 resulted in midgestational lethality with a complete absense of fetal liver hematopoiesis during murine development, while no effect was observed on the primitive yolk sac-derived erythropoiesis [10,11]. It was also proved that the null mutations in mouse Runx1 completely abolished the transition of the first definitive HSC from haemogenic endothelial cells at the AGM region [12,13]. In contrast with its critical role during development, Runx1 is not necessary for the maintenance of HSC in adult hematopoiesis, but it is required for differentiation and maturation of some hematopoietic lineage. For example, hematopoietic progenitors were fully maintained in the Runx1 mutant mice, and most myeloid progenitors lacking Runx1 could still differentiate into mature neutrophils [14]. Runx3 served partial overlapping functions with Runx1 in the homeostatic maintenance of HSC [1,15]. The functional redundancy between Runx1 and Runx3 was unveiled by the lethality in Runx1:Runx3 double-knockout (DKO) mice due to bone marrow failure. Moreover, it also caused multiple differentiation blocks and stem cell exhaustion, which were not observed in the respective single conditional knockout mice [15]. In addition to hematopoiesis, Runx proteins participate in innate immunity by regulating cytokine production. For example, Runx1 was reported to be involved in innate immunity such as regulating IL4 silencer to repress IL4 gene in naive CD4 + T cells [16]. In the presence of the pro-inflammatory cytokines TNF-α and IL-1, Runx3 strongly augmented the secretion of IL23A, a subunit of IL-23, which was best known as pro-inflammatory cytokine to drive Th17 activities [17,18].

Runx paralogs-homologs have also been studied in several invertebrates, most notably in the fruit fly *D. melanogaster*. Up to date, single Runx gene has been found in most of the studied invertebrates, which is significant different from mammals [19,20]. For example, only one Runx gene has been reported from sea squirt *Ciona intestinalis* [19], sea urchin *Strongylocentrotus purpuratus* [21], scallop *Chlamys farreri* [22,23], and the nematode *Caenorhabditis elegans* [24], respectively. However, three and four Runx genes were identified from mosquito *Anopheles gambiae* [19] and *D. melanogaster*, respectively [25]. It is worth noting that there is no overlap for the functions of Runx genes in all the investigated invertebrates [20]. So far, the roles of Runx proteins were only investigated in several invertebrate model organisms. For example, there are two Runx genes annotated in *S. purpuratus* genome, while only SpRunt-1 has been confirmed to mainly regulate differentiation as well as proliferation during the sea urchin embryogenesis [21,26,27]. The sole *C. elegans* rnt-1 is a core component in the regulation of the division pattern of seam stem cells [26]. There are four Runx genes identified in *D. melanogaster*, and Lozenge is the single Runx gene involved in hematopoiesis [28]. About 60% of prohaemocytes with lozenge expressed at seven to nine larval stages would differentiate into mature crystal cells, while no crystal cells appeared in the lozenge mutants [28,29]. While the information about another two Runx genes CG34145 (also known as Runt related A) and CG42267 (also known as CG15455 or Runt related B) is still very limited. Recently, Runx (*Cf*Runt) was proved to play essential roles in regulating hemocyte production of scallop *C. farreri*. After knock-down of *Cf*Runt, the hemocyte renewal rates and circulating total hemocytes count both decreased significantly [22].

Hemocytes, as the effective immunocytes in invertebrates, take part in numerous key immune processes, such as phagocytosis, nodule, and encapsulation [30]. However, the origin and development of hemocytes is still unknown in molluscs and current knowledge about mollusc hematopoiesis is very limited. In adult oyster, a population of adult somatic precursor cells was reported in gills, and they were found to differentiate into hemocytes [31]. The larval hematopoiesis of molluscs has been investigated in the mussel *Mytilus edulis*, European flat oyster *Ostrea edulis* and scallop *C. farreri* by using the monoclonal antibody against adult hemocytes [32–34]. The positive signals were detected as early as D larval stage (48 hpf), and the hematopoietic tissue was reported to locate at the vesicle tissues around adductor in juvenile scallop, which was consistent with the observation in adults [34]. However, the application of monoclonal antibody against adult hemocytes in larval or newborn hemocytes would be a challenge because of different degrees of differentiation. Recently, more orthologous of conserved hematopoietic transcription factors were identified in the molluscs, such as SCL, GATA3 and CBFβ [22,35,36], which would provide new methods to explore the hematopoiesis.

The Pacific oyster *Crassostrea gigas* is one of the most commercially and ecologically important bivalves worldwide. In the present study, a conserved hematopoietic transcription factor *Cg*Runx was identified from *C. gigas*. It was specifically expressed in the hemocytes as well as the potential hematopoietic related tissues gill and mantle. It was further demonstrated that *Cg*Runx involved in immune response and might participate in larvae hematopoiesis in oyster.

2. Materials and methods

2.1. Animals and immune challenges

Pathogenic bacteria *Vibrio splendidus* [37,38] was cultured in 2216E media (5 g/L Tryptone, 1 g/L Yeast extract, 0.1 g/L Ferric phosphate in seawater) at 16 °C for 24 h and harvested by centrifuged at 3000 *g*, 4 °C for 10 min. The pellet was washed three times and re-suspended in 1 × PBS (137 mM NaCl, 2.7 mM KCl, 4.3 mM Na_2HPO4, 1.4 mM KH_2PO4, pH 7.4) at a final concentration of 2×10^8 CFU/ml.

Adult Pacific oyster *C. gigas*, with an average shell length of 13.0 cm, were collected from the commercial farm in Dalian, China, and acclimated in aerated seawater at 23 °C for seven days prior to use. One hundred and eighty oysters were randomly divided into three groups. The oysters in the control group received an injection of 100 μL PBS. The oysters in the treatment groups received an injection of 100 μL lipopolysaccharides (LPS, 1 mg/mL in PBS) from *Eschenchia coli* 0111:B4 (Sigma, L2630) and 100 μL V. *splendidus*, respectively. Nine oysters were randomly sampled from each group at 0, 3, 6, 12, 24, 48 and 72 h after injection. The samples from three oysters were mixed up randomly as one replicate, and there were three replicates for each time point. The hemolymphs were extracted from the hematococoel using a sterile syringe with pre-cooled modified Alsever's solution (MAS, 20.8 g/L glucose, 8.0 g/L sodium citrate, 3.36 g/L ethylene diamine tetraacetic acid, 22.5 g/L sodium chloride, pH 7.5) at the ratio of 1:1. After centrifugation at 4 °C, 800 *g* for 10 min, the hemocyte pellets were used for immunofluorescence staining and mRNA extraction. Meanwhile, different tissues (mantle, gonad, gill, gland, and adductor muscle) obtained from six adult oysters, were used for mRNA extraction and immunofluorescence staining.

2.2. Larvae collection

The oyster embryo and larvae were reproduced in Changhai oyster hatchery, and the detailed procedures about the oyster larval rearing were referred to previous reports [39]. To analyze the expression pattern of *CgRunx* during development, larvae were sampled at 12 different developmental stages, including Zygote (0.5 h post fertilization, hpf), 2 cell embryos (1.5 hpf), 8 cell embryos (2 hpf), Morula (3 hpf), Blastula (4 hpf), early Gastrula (5 hpf), Gastrula (8 hpf), early Trochophore (10 hpf), Trochophore (15 hpf), D-veliger larvae 1 (22 hpf), D-veliger larvae 2 (72 hpf), and early Umbo larvae (120 hpf). They were fixed for whole-mount immunofluorescence assay or directly stored at −80 °C.

For whole-mount immunofluorescence assay, the embryo and larvae before Trochophore stage were directly fixed in pre-cooled 4% paraformaldehyde (PFA, Sangon Biotech, E672002) at 4 °C for 16 h, while larvae older than 24 hpf were firstly relaxed by gradual addition of 7.5% $MgCl_2$ (7.5 g in 100 ml filtered seawater) and then fixed as above description. After fixation, all samples were washed with PBS for two times, and then dehydrated in gradient methanol-PBS solutions (25%,

Table 1
Primers used in this study.

Primer name	Primer sequences(5′-3′)	Primer purpose
oligo (dT)-adaptor	GGCCACGCGTCGACTAGTACT	Adaptor primer
M13-47	CGCCAGGGTTTTCCCAGTCACGAC	Sequencing primer and individual bacterial colonies PCR
RV-M	GAGCGGATAACAATTTCACACAGG	
T7-F	TAATACGACTCACTATAGGG	
T7-R	TGCTAGTTATTGCTCAGCGG	
*Cg*Runx-F	AACCACATGCATTTACCTACAG	Gene clone
*Cg*Runx-R	TCAATATGGCCGCCAAAC	
Re-*Cg*Runx-F	GGGGTAC/CTCCCCCCACAATATGTC	Recombination primers
Re-*Cg*Runx-R	CGGAATTC/ TGACTTTACTGCGAGGGTC	
RT-*Cg*EF-F	AGTCACCAAGGCTGCACAGAAAG	RT-PCR
RT-*Cg*EF-R	TCCGACGTATTTCTTTGCGATGT	
RT-*Cg*RS18-F	GCCATCAAGGGTATCGGTAGAC	
RT-*Cg*RS18-R	CTGCCTGTTAAGGAACCAGTCAG	
RT-*Cg*Runx-F	CGCAAAGAGCGGACGGAAC	
RT-*Cg*Runx-R	ATTTGTAGAGGGATATGGCGGTAA	

50%, 75%), and finally stored in 100% methanol at −20 °C.

2.3. Gene cloning and sequence analysis

Total mRNA was extracted from larvae (about 1×10^5) and tissues using TRIzol™ reagent according to the manufacture's protocol (Thermo Fisher Scientific, 15596026). The first-strand synthesis was carried out based on M-MLV RT Usage information using the DNase I (Promega, M610A)-treated total RNA as template and oligo (dT)-adaptor as primer (Table 1). Specific primers *Cg*Runx-F and *Cg*Runx-R (Table 1) were designed based on the predicted *Cg*Runx gene (GenBank accession number: LOC105336942) to clone the complete open reading frame (ORF) of *Cg*Runx from *C. gigas*. The cDNA of hemocytes was served as PCR template. The PCR products were purified and confirmed through sequencing with primers M13-47 and RV-M (Table 1) after they were inserted into pMD™19-T Vector (Takara, 6013) and transformed into competent cells of *Escherichia coli* Trans5α (TransGen Biotech, CD201-01). The homology search of the Runx family was conducted by BLAST algorithm at the NCBI. Multiple alignment of the deduced amino acid sequences of *Cg*Runx and other Runx was performed with the ClustalW multiple alignment program (http://www.ebi.ac.uk/clustalw/). Bioedit 7.0 was used to align the conserved Runt domains with other known Runx sequences and to calculate their sequence similarities [40]. The deduced amino acid sequences were analyzed with the Expert Protein Analysis System (http://www.expasy.org) and simple modular architecture research tool (SMART) version 5.1 (http://smart.embl-heidelberg.de/) [41]. The potential NLS motif was predicted *via* NLStradamus (http://www.moseslab.csb.utoronto.ca/NLStradamus/) [42].

2.4. Recombinant expression and purification of CgRunx protein

The runt domain of *CgRunx* was amplified by using primers Re-*Cg*Runx-F and Re-*Cg*Runx-R (Table 1). The PCR product of 453 bp with Kpn I and EcoR I sites (nucleotides 38–490) was cloned into the Kpn I/EcoR I sites of expression vector pET-30a (+) (Novagen, 69909-3). The recombinant plasmid pET-30a (+)-*Cg*Runx was transformed into *E. coli* transetta (DE3) chemically competent cell (TransGen Biotech, CD801-01), and the pET-30a (+) vector without insert fragment was used as negative control. Positive clones were screening by monoclonal colony PCR and confirmed by sequencing with primers T7-F and T7-R (Table 1). Positive cells were incubated in LB liquid medium at 37 °C containing kanamycin (100 μg/mL). The recombinant protein r*Cg*Runx was induced by adding isopropyl-β-d-thiogalactoside (IPTG) to a final concentration of 0.5 mM when the cells grew to OD600 = 0.5, and the cells were incubated for additional 4 h to express sufficient protein. r*Cg*Runx was purified through the Ni-Sepharose FF (Beijing Wei shi bo hui chromatographic technolog co.LTD, CS-A01b), quantified by Bicinchoninic acid (BCA, Beyotime, P0009) method [43], and stored at −80 °C for subsequent experiment.

2.5. Preparation of antibody and western blotting analysis

To prepare antibody against *Cg*Runx, the re-natured r*Cg*Runx protein was dialyzed against deionized water. Three 6-weeks female rat were immuned by r*Cg*Runx (1 μg/μl) to acquire polyclonal antibody according to the previous method [44]. Briefly, three 6-weeks female rat were acclimated in lab for seven days prior to use. On day 1, three 6-weeks female rat were inoculated intraperitoneally with 100 μg of r*Cg*Runx with an equal part of complete Freund's adjuvant (Sigma, F5881). On day 15, booster immunizations were given to each rat with 100 μg of r*Cg*Runx in incomplete Freund's adjuvant (Sigma, F5506) intraperitoneally. On days 22 and 30, booster injections were given twice by tail vein with 50 μg of r*Cg*Runx. Seven days after the last injection, the blood was drawn from the posterior venous plexus of rat and obliquely placed at 4 °C overnight. The immune serum (containing anti-*Cg*Runx antibody) was collected after centrifugation at 4 °C, 3000 *g* for 30 min, and then directly used to test the specificity of anti-*Cg*Runx antibody by Western blot analysis. Briefly, r*Cg*Runx were separated by 12% SDS-PAGE and electrophoretically transferred onto a sheet of PVDF (polyvinylidene fluoride) membrane. After blocked in blocking solution (3% skim milk powder dissolved in TBST) at room temperature (RT) for 2 h, the membrane was incubated with anti-r*Cg*Runx antibody diluted to 1:1000 (v/v) in blocking buffer at 4 °C overnight, and then incubated with 1:2000 (v/v) HRP (horseradish peroxidase)-conjugated anti-rat IgG for 1 h. All the incubation was performed at RT and followed by three times of washing with TBST (8.8 g/L NaCl, 2.4 g/L Tris Base, 1.3 ml/L HCl, 1 ml/L Tween-20, pH 7.4). The membrane was finally incubated with ECL detection reagents (Thermo Fisher Scientific, WB7106) after repeated heavily washing with TBST for three times, and then exposed to film for 3 min.

2.6. Immunofluorescence assay

Immunofluorescence assays of larval in different developmental stages and adult tissues were referred to the previous reports with minor modification [45]. Briefly, the larvae were rehydrated in gradient methanol-PBS solutions (75%, 50%, 25%, and PBS) and the shelled larvae (1 day and up) were decalcified with 5% EDTA in PBS (5 g EDTA in 100 ml PBS). After blocked in blocking solution (10% normal goat serum, 3% bovine serum albumin in PBS) at RT for 2 h, the larvae were incubated with the anti-*Cg*Runx antibody (1:1000 dilutions in blocking solution) at 4 °C overnight. These specimens were then washed (3 × 20 min) in PBST (containing 0.1% Tween-20, v/v) and incubated with a mixture of goat anti-rat IgG conjugated to Alexa Fluor 488 (1:1000 dilutions in blocking solution; Thermo Fisher Scientific, Z25002) at RT for 2 h.

The tissues were fixed in Bonin's fixative (saturated solution of picric acid: formaldehyde: glacial acetic acid = 15:5:1) at RT for 24 h, decolored (4 × 2 h) in 70% ethanol, and dehydrated in gradient ethanol-distilled water solutions (80%, 95% and 100%). After soaked twice in xylene, the samples were embedded in paraffin. Cross-sections of 5 μm thick were sliced and dried at 56 °C overnight. The Paraffin was eliminated with xylene solution and the sections were then rehydrated in gradient ethanol-distilled water solutions (95%, 80%, 70%, 50% and 30%), and eventually in distilled water. The histological sections of different tissues were incubated at 58 °C for 1 h and washed with PBST for 5 min, and the antigen of sections were retrieved by 0.01 M citrate buffer (2.38 μg/L $Na_3C_6H_5O_7{\cdot}2H_2O$, 0.4 μg/L $C_6H_5O_7{\cdot}H_2O$, in 200 ml distilled water) at 120 °C for 6 min. The hemocytes were collected as previously described above. After centrifugation at 4 °C, 800 *g* for 10 min, the hemocyte pellets were re-suspend in modified L-15 medium

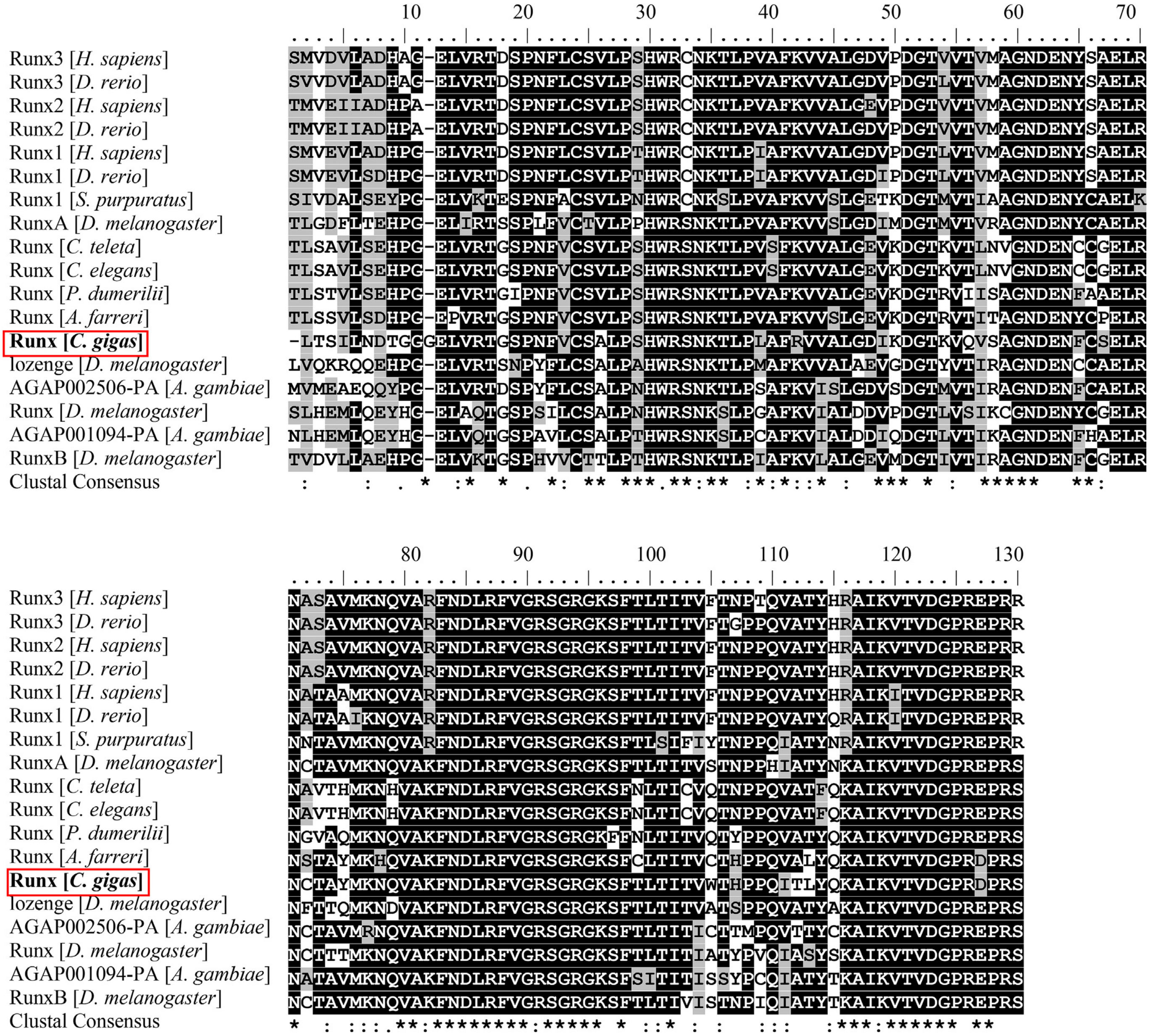

Fig. 1. Multiple alignments of the runt domain of *Cg*Runx with other Runt-related transcription factors from various species. The black shadow region means all sequences share the same amino acid residue, and the grey shadow indicates the amino acids with similarity more than 50%. Gaps are indicated by dashes to improve the alignment. "*" indicates positions which have a single, fully conserved residue. ":" indicates that one of the following 'strong' groups is fully conserved. "." indicates that one of the following 'weaker' groups is fully conserved. Proteins analyzed list below: Runx1 [*Homo sapiens*]: XP_011528068.1; Runx2 [*Homo sapiens*]: NP_001019801.3; Runx3 [*Homo sapiens*]: NP_001307601.1; Runx1 [*Danio rerio]*: NP_571678.1; Runx2 [*Danio rerio*]: NP_998023.1; Runx3 [*Danio rerio*]: NP_571679.2; Runx1 [*Strongylocentrotus purpuratus*]: NP_999779.1; lozenge [*Drosophila melanogaster*]: AAF35308.1; Runt [*Drosophila melanogaster*]: NP_523424.2; RunxA [*Drosophila melanogaster*]: ABI30990.2; RunxB [*Drosophila melanogaster*]: NP_001259745.1; *Cf*Runt [*Chlamys farreri*]: AGI44582.1|; *CgRunx* [*Crassostrea gigas*]: EKC36272.1; Runx [*Platynereis dumerilii*]: AGS55453.1; Runt related [*Caenorhabditis elegans*]: NP_491679.1; AGAP001094-PA [*Anopheles gambiae str.* PEST]: XP_001689117.2; AGAP002506-PA [*Anopheles gambiae str.* PEST]: XP_312433.5.

(M-L15, supplemented with 0.54 g/L KCl, 0.6 g/L $CaCl_2$, 1 g/L $MgSO_4$, 3.9 g/L $MgCl_2$, 20.2 g/L NaCl) and deposited on the clean Poly-L-Lysine pre-coated slides (Sangon Biotech, E678002) in the wet chamber for 1 h. Then the hemocytes were fixed with pre-cooled 4% PFA (Sangon Biotech, E672002) for 1 h, and washed three times with PBST. The slides were per-meabilized with PBST for 10 min, and washed with PBST for three times. The following operations were the same as above and processed with blocking, incubation with primary and secondary antibodies, sequentially, and the cell nucleuses were stained by DAPI (Beyotime, C1002). The samples incubated with anti-His-tag antibody plus secondary antibody was used as negative control.

After dehydrated with a series of isopropanol washes, all samples were cleared and mounted in Murray's clear (1:2 benzyl alcohol and benzyl benzoate) [46] and examined using the Zeiss Laser-Scanning Confocal Microscopy System LSM 710 (Zeiss, 710).

2.7. Quantitative real-time polymerase chain reaction (qRT-PCR) analysis

The mRNA transcripts of *CgRunx* were examined by qRT-PCR to quantify the expression levels in different developmental stages and tissues, as well as the expression in hemocytes after bacterial challenge. Total mRNA was extracted as previous description, and the cDNA synthesis was carried out according to the manufacture's protocol of PrimeScript™ RT reagent kit (TaKaRa, RR037A). The reaction mixtures (including Enzyme Mix, cDNA and primers) were incubated at 42 °C for 1 h, and terminated by heating at 95 °C for 5 min. The cDNA mix was diluted to 1:50 and subsequently performed qRT-PCR.

qRT-PCR was carried out using a Light Cycler 7500 Real-Time PCR System (Applied Biosystems® Life Technologies) with SYBR Green as the fluorescent dye according to the manufacturer's protocol (TaKaRa, RR820L). The thermal program was as follows: denaturation at 94 °C for 15 s, followed by 40 cycles at 94 °C for 15 s, 60 °C for 30 s. The relative gene expression levels of target genes during early development stages and different tissues in adult oysters were normalized to the expression of *CgRS-18* and *CgEF-1α*, respectively, and determined by the typical Ct method ($2^{-\triangle\triangle Ct}$ method) [47]. All primers (RT-*Cg*EF-F and RT-*Cg*EF-R, RT-*Cg*RS18-F and RT-*Cg*RS18-R, RT-*Cg*Runx-F and RT-*Cg*Runx-R) used in this assay were listed in Table 1. There were three biological replicates for each group. Data were analyzed by using ANOVA and Student's t-test. Differences were considered significant as $p < 0.05$. All results were represented as mean ± standard error.

3. Results

3.1. The phylogeny and multiple sequences alignment of CgRunx

A nucleotide sequence of 1638 bp representing the complete coding sequence (CDS) of Runx orthologs (named as *Cg*Runx) was cloned from Pacific oyster *C. gigas*, which encoded a polypeptide of 545 amino acids with the predicted molecular weight of 60.8 kDa and theoretical isoelectric point of 8.098. The deduced amino acid sequence of *Cg*Runx contained a 128 well-conserved runt homology domain in the N-terminal region (30–158), a nuclear localization signal (NLS, 153 -PRDPRSKVKLRT- 164), and a C-terminal VWRPY motif (Fig. S1). The homology search of the protein sequences of *Cg*Runx was conducted by BLASTP. Multiple sequences alignment of *Cg*Runx with other Runt-related transcription factors revealed that *Cg*Runx shared 81% similarity with Runt from scallop *C. farreri* (Accession No. AGI44582.1), 77% similarity with lozenge from fruit fly *D. melanogaster* (Accession No. AAF35308.1), and 63%–75% with Runx 1 (Accession No. XP_011528068.1), Runx 2 (Accession No. NP_001019801.3) and Runx 3 (Accession No. NP_001307601.1) from human *Homo sapiens*, Runx 2 (Accession No. NP_998023.1) from zebrafish *Danio rerio*, SpRunt-1 from sea urchin *S. purpuratus*, Runt (Accession No. NP_523424.2) and runt related A (Accession No. ABI30990.2) from *D. melanogaster* (see Fig. 1).

3.2. Spatio-temporal expression of CgRunx mRNA in C. gigas

In adult oyster, the mRNA transcripts of *CgRunx* could be detected in all the examined tissues. The expression level of *CgRunx* was highest in the hemocytes, which was 64.35-fold of that in adductor muscle ($p < 0.05$). It was also higher in gill, mantle, and gonad (13.55-, 8.52- and 6.93-fold, respectively) ($p < 0.05$). The expression level of *CgRunx* in gland was almost the same as that in adductor muscle (Fig. 2A).

The mRNA expression of *CgRunx* was examined in the embryo and larvae of different developmental stages. The mRNA expression level was low in the newly fertilized eggs, increased gradually to a relative high level during the 8 cell embryos and Blastula stages (2–4 hpf, about 40-fold), and peaked at early Trochophore larvae (10 hpf, about 60-fold). It decreased dramatically in the Trochophore larvae (15 hpf) and then resumed after entering into D-veliger and Umbo larvae (Fig. 2B).

3.3. The prokaryotic expression of CgRunx and western blot analysis

The recombinant protein of *Cg*Runx was expressed in *E. coli* transetta (DE3) and purified by the His-tag Protein Fusion and Purification System. Distinct bands of ~37 kDa and ~60 kDa were observed both in SDS-PAGE and Western blot analysis (Figs. S2A and S2B), which were consistent with the predicted molecular mass of r*Cg*Runx (~37 kDa) and *Cg*Runx (~60.8 kDa), respectively, indicating the specificity of anti-*Cg*Runx.

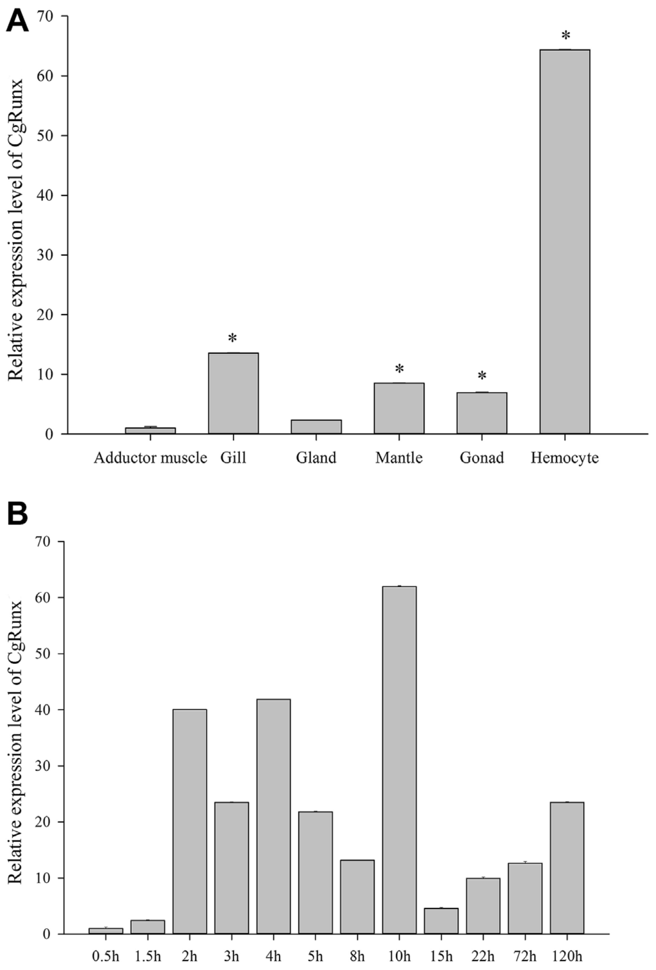

Fig. 2. The expression pattern of *CgRunx* in different tissues (A) and developmental stages (B). 0.5 hpf: Zygote; 1.5 hpf: 2 cell embryos; 2 hpf: 8 cell embryos; 3 hpf: Morula; 4 hpf: Blastula; 5 hpf: early Gastrula; 8 hpf: Gastrula; 10 hpf: early Trochophore; 15 hpf: Trochophore; 22 hpf: D-veliger larvae 1; 72 hpf: D-veliger larvae 2; 120 hpf: early Umbo larvae. The relative *CgRunx* expression levels in different tissues and developmental stages were normalized to the expression of *CgEF-1α* and *Cg18S*, respectively. Date was shown as mean ± S.E (n > 3). Statistically significant differences were designated at $p < 0.05$.

3.4. Distribution of CgRunx in different tissues of adult C. gigas

The distribution of *Cg*Runx was observed in six tissues of *C. gigas* using immunofluorescence technique. The positive signals of *Cg*Runx protein were of green fluorescence, and it was clearly observed in the hemocytes, mainly in the cell nucleus. The immunopositive fluorescence appeared in the gill filaments and specialized at the tubule lumen region. Moreover, the positive immunofluorescence signals also occurred in the mantle tissue and distributed in the wrinkles of mantle edge (Fig. 3). Although the expressions of *CgRunx* mRNA were detected in gland, gonad and adductor muscle, there were almost no positive signals of *Cg*Runx protein detected in these tissues (Fig. S3). In addition, there was no immunoreactivity fluorescence in negative controls of all the tested tissues (Fig. S4).

3.5. The spatial expression of CgRunx during C. gigas ontogenesis

The spatial expression of *Cg*Runx during *C. gigas* ontogenesis was

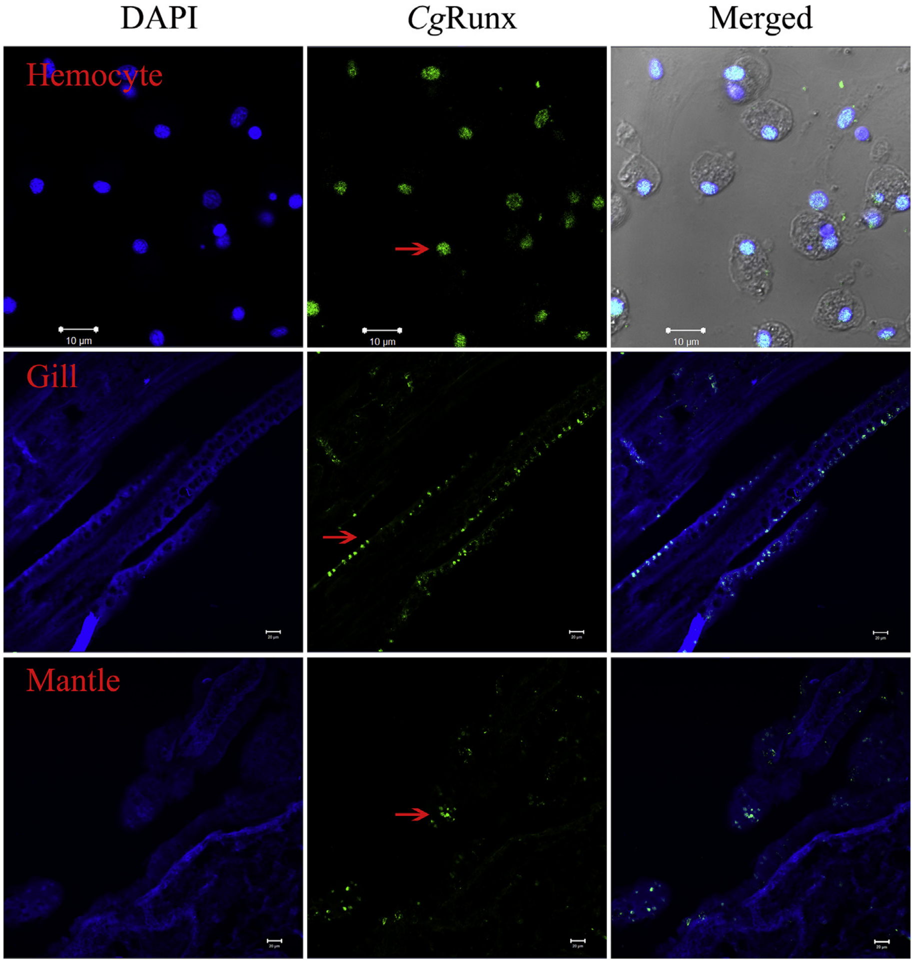

Fig. 3. Immunofluorescence of *CgRunx* in hemocyte, gill and mantle tissues. The red arrow indicate positive signal. The scale bar is 10 μm (hemocyte) and 20 μm (gill and mantle), respectively. (For interpretation of the references to color in this figure legend, the reader is referred to the Web version of this article.)

investigated at six different stages by using whole-mount immunofluorescence assay. The positive signals of *Cg*Runx protein were observed in all the six examined larvae stages (Fig. 4). The immunopositive spots were distributed abundantly through the whole embryo at Blastula stage (5 hpf), while the distributions were specialized gradually to the vegetal pole cells in Gastrula (8 hpf), and progressively reduced with development to a ring structure around the dorsal region in Trochophore larvae (beginning at 10 hpf). In D-veliger larvae, the scattered positive immunofluorescence signals appeared in the velum region. A specific sinus structure was observed on the dorsal side in the early D-veliger larvae (D-veliger 1), while the immunofluorescence signals of *Cg*Runx could be detected as fibrillary structure through the whole larvae body in the D-veliger 2 larvae. The expression pattern lasted and even became stronger until in the Umbo larvae (Fig. 4). In addition, there was no immunoreactivity fluorescence in negative controls of all the six larval stages (Fig. S5).

3.6. Temporal expression of CgRunx in hemocytes after immune challenge

The expressions of *CgRunx* mRNA in hemocytes after the stimulations of LPS and *V. splendidus* were examined by qRT-PCR. The expression levels of *CgRunx* in the hemocytes were significantly upregulated at 3 h after LPS stimulation (2.98-fold, $p < 0.05$), and maintained a high expression level through the whole challenge period (6 h: 2.67-fold, $p < 0.05$; 12 h: 2.36-fold, $p < 0.05$; 24 h: 3.76-fold, $p < 0.05$; 48 h: 1.41-fold, $p < 0.05$; 72 h: 1.86-fold, $p < 0.05$), compared to that in the PBS control group (Fig. 5).

After the immune challenge with *V. splendidus*, the mRNA transcripts of *CgRunx* in hemocytes increased 2.46, 1.5 and 1.38-fold at 3 h, 6 h and 12 h after challenge, respectively. The mRNA transcripts of *CgRunx* were significantly re-upregulated at 72 h after *V. splendidus* challenge, which was 2.06-fold ($p < 0.05$) higher than that in the PBS control group (Fig. 5).

4. Discussion

Runx transcription factors are defined by the presence of a runt domain and represented by Runx1, Runx2 and Runx3 in mammals [1]. Among their diverse roles as transcriptional regulators during development and cell fate specification, the Runx transcription factors (Runx1 and Runx3) are best known for their involvements in hematopoiesis [10,11,13,15]. In the present study, a conserved transcription factor of Runx family, *Cg*Runx, was characterized in oyster *C. gigas*. There was a conserved runt domain in *Cg*Runx, which shared highly identity with that in other Runx transcription factors, especially with *Cf*Runt from scallop, lozenge from fruit fly, and mammal Runx3. It was consistent with the hypotheses that the evolution of invertebrates Runx gene was considered to begin with the smallest vertebrate Runx gene, Runx3 [48]. These results strongly suggested that *Cg*Runx belonged to the typical runt domain family of transcription factors, and might preferentially preserve conservative function in hematopoiesis and immune system as Runx orthologs in mammals.

As hematopoietic transcription factors, Runx1 and Runx3 are mainly expressed in hematopoietic tissues and multi-lineage blood cells in vertebrates to regulate cell-specific gene expression [1,8]. In the present study, *Cg*Runx was highly expressed in the hemocytes both at

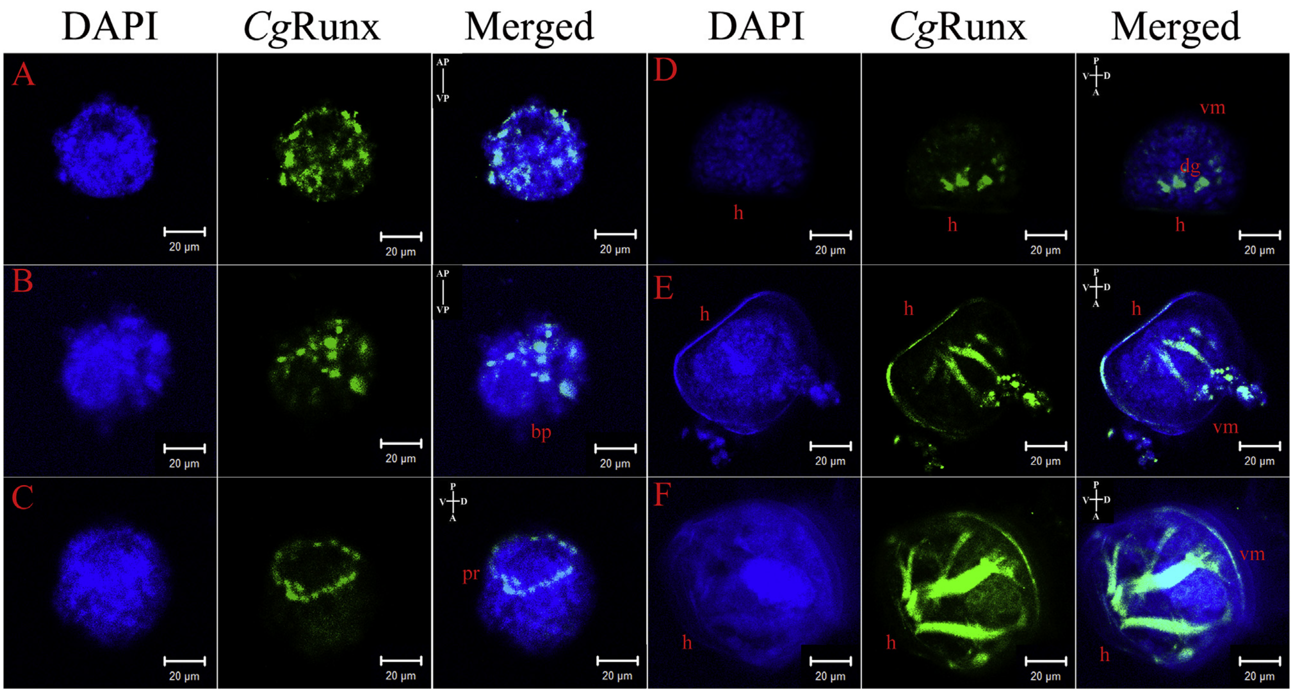

Fig. 4. Whole-mount immunofluorescence of *Cg*Runx in *C. gigas* larvae. The positive signals of *Cg*Runx are in green. A: Blastula, 4 hpf; B: Gastrula, 8 hpf; C: Trochophore, 15 hpf; D: D1: D-veliger larvae 1, E: 22 hpf; D2: D-veliger larvae 2, 50 hpf; F: Early umbo larvae, 120 hpf. bp: blastopore. dg: digestive gland; h: hinge; pr: prototroch; vm: velum; AP: Animal pole; VP: vegetal pole; A: anterior; D: dorsal; P: posterior; V: ventral. The scale bar is 20 μm. (For interpretation of the references to color in this figure legend, the reader is referred to the Web version of this article.)

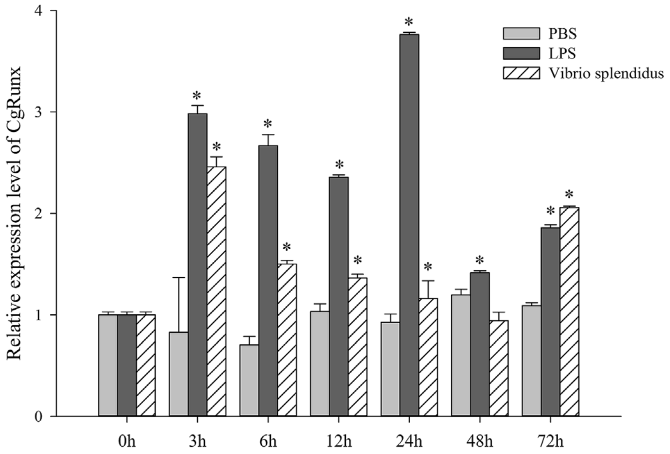

Fig. 5. Temporal mRNA expression patterns of *CgRunx* in hemocytes after LPS and *V. splendidus* stimulation. The relative *CgRunx* expression levels were normalized to the expression of *CgEF-1α* and determined for each group. The final values were shown as mean ± SD, N = 3. Statistically significant differences were designated at $p < 0.05$.

the protein and nucleic acid levels, and relatively higher in potential hematopoietic organ gill and mantle. Immunofluorescence staining showed that *Cg*Runx was located in the nucleus of hemocytes. It was also distributed at the tubule lumen of gill, and the wrinkles of mantle, which was corroborated with the results of qRT-PCR assay. Recently, gill was considered to be a predominant tissue participating in the hematopoiesis and immune response in adult oyster [31,49]. Histochemistry and immunofluorescence assays revealed that the stem-like cells with big nuclei and thin cytoplasm were observed in the tubules of gill filaments, where DNA synthesis was active and hemocytes production were exuberant [49]. Besides, several pattern recognition receptors and hematopoietic transcription factors specially expressed in hemocytes, such as *Cg*Clec-4, *Cg*GATA2/3 and *Cg*SCL, were also found to be expressed in the gill filaments, signifying that hemocytes were rich in the gill tissue of oyster [35,36,49]. Increasing evidences showed that mantle might be another hematopoietic site or storage center for hemocytes in bivalves. For example, hemocytes were observed in the tissues of gill and mantle of scallop *C. farreri* [50]. Moreover, more evidences demonstrated that hemocytes (mainly granulocytes) directly participated in the synthesis and delivery of $CaCO_3$ crystals during shell regeneration process [51,52]. The expression of *Cg*Runx mRNA in hemocytes was significantly up-regulated after LPS and *V. splendidus* stimulations, indicating its involvement during immune response, which was consistent with the additional role for Runx1 and Runx3 in the innate immunity [16,17]. The unique expression pattern of *Cg*Runx in hemocytes as well as the potential hematopoiesis sites in gill and mantle suggested the potential role of *Cg*Runx in oyster hematopoiesis.

The initiation of hematopoiesis is a critical event during the immune system ontogeny in most organisms, and the evolutional conserved hematopoietic transcription factors are usually used to explore the development of hematopoietic system [53]. As a pivotal factor in HSC ontogeny, Runx1 and Runx3 are expressed in all the sites for hematopoietic cells emergence, and its expression marks the long-term repopulating of HSCs in the midgestation mouse embryo [1,8]. In the present study, *Cg*Runx was investigated during ontogenesis of oyster to identify the potential origin site and developmental pattern of hematopoiesis. Similar with the *Cf*Runt in scallop [23] and *Sp*Runt in sea urchin [21], *Cg*Runx protein was found to distribute throughout the whole embryo at Blastula and Gastrula stages in oyster. *Sp*Runt was reported to be associated with terminal differentiation in all major tissue territories during embryogenesis of sea urchin [26]. The present results indicated that the abundant expression of *Cg*Runx in early embryo might be necessary for the polarity establishment and cell fate determination of oyster embryo. The specialized expression patterns of *Cg*Runx in Trochophore and D-veliger larvae were quite similar to that of another two highly conserved hematopoiesis transcription factors *Cg*GATA2/3 and *Cg*SCL revealed by whole mount *in situ* hybridization and immunofluorescence [35,36]. GATA3 and SCL are another two conserved transcription factors involved in hemopoietic regulation, which have been well documented in vertebrates, as well as some invertebrates such as sea urchin, fruit fly, scallop, and oyster [54,55]. Genomics and chromatin analysis revealed that a highly conserved 531-bp enhancer was located at the first intron of mouse Runx1 gene, which was crucial for the early hematopoietic expression of Runx1, and targeted all definitive HSCs in the mouse embryo [56]. *In vivo* binding assay of transcription factor and analysis of the mutated enhancer implicated that GATA2 and SCL proteins were critical factors for Runx1 function. The GATA/Ets/SCL protein complex was recruited to the enhancer of Runx1 *in vivo* to initiate HSC generation together [56,57]. In the present study, the similar expression patterns of these three conserved transcription factors supported that the ring structure around the dorsal region of embryo should be the potential site of hematopoiesis in Trochophore larvae of oyster, and *Cg*Runx might participate in larvae hematopoiesis.

In conclusion, the transcription factor *Cg*Runx was found to be highly conserved across species and specifically expressed in the important immune organs such as gill, mantle, and hemocytes. The expression levels of *CgRunx* transcripts were significantly up-regulated under the stimulations of LPS and *V. splendidus*, suggesting its immune role in oyster. During the developmental stages, the mRNA abundance of *Cg*Runx increased gradually after newly fertilization and reached the peak value at Trochophore stage. The expression pattern of *Cg*Runx suggested that it might involve in larvae hematopoiesis of the Pacific oyster. Above results collectively suggested that *Cg*Runx preferentially preserved conservative function in hematopoiesis and immune system as Runx orthologs in mammals.

Acknowledgements

The authors thank all members in Dr. Song's laboratory for valuable discussions. This research was supported by a grant from National key R &D Program of China (201)8YFD0900502), National Science Foundation of China (U1706204), Key R&D Program of Liaoning Province (2017203004 to L. S.), Distinguished Professor of Liaoning (to L. S.), Climbing scholars of Liaoning (to L. S.), Dalian High Level Talent Innovation Support Program (2015R020), the Research Foundation for Aoshan Talent Cultivation Program Supported by Qingdao National Laboratory for Marine Science, Earmarked Fund (CARS-49) from Modern Agro-industry Technology Research System, and Technology and Talented Scholars in Dalian Ocean University, and Natural Science Foundation of Liaoning, China (20170520056).

Appendix A. Supplementary data

Supplementary data to this article can be found online at https://doi.org/10.1016/j.fsi.2019.03.066.

References

[1] D.C. Voon, Y.T. Hor, Y. Ito, The RUNX complex: reaching beyond haematopoiesis into immunity, Immunology 146 (2015) 523–536.
[2] J.P. Gergen, B.A. Butler, Isolation of the Drosophila segmentation gene runt and analysis of its expression during embryogenesis, Genes Dev. 2 (1988) 1179–1193.
[3] J.B. Duffy, M.A. Kania, J.P. Gergen, Expression and function of the Drosophila gene runt in early stages of neural development, Development (Cambridge, England) 113 (1991) 1223–1230.
[4] J.B. Duffy, J.P. Gergen, The Drosophila segmentation gene runt acts as a position-specific numerator element necessary for the uniform expression of the sex-determining gene sex-lethal, Genes Dev. 5 (1991) 2176–2187.
[5] E. Dzierzak, N.A. Speck, Of lineage and legacy: the development of mammalian hematopoietic stem cells, Nat. Immunol. 9 (2008) 129–136.
[6] K. Morita, C. Tokushige, S. Maeda, H. Kiyose, M. Noura, A. Iwai, et al., RUNX transcription factors potentially control E-selectin expression in the bone marrow vascular niche in mice, Blood Adv. 2 (2018) 509–515.
[7] J.W. Wang, S. Stifani, Roles of Runx genes in nervous system development, Adv. Exp. Med. Biol. 962 (2017) 103–116.
[8] T.E. North, M.F. de Bruijn, T. Stacy, L. Talebian, E. Lind, C. Robin, et al., Runx1 expression marks long-term repopulating hematopoietic stem cells in the midgestation mouse embryo, Immunity 16 (2002) 661–672.
[9] T. North, T.L. Gu, T. Stacy, Q. Wang, L. Howard, M. Binder, et al., Cbfa2 is required for the formation of intra-aortic hematopoietic clusters, Development (Cambridge, England) 126 (1999) 2563–2575.
[10] Z. Cai, M. de Bruijn, X. Ma, B. Dortland, T. Luteijn, R.J. Downing, et al., Haploinsufficiency of AML1 affects the temporal and spatial generation of hematopoietic stem cells in the mouse embryo, Immunity 13 (2000) 423–431.
[11] T. Okuda, J. van Deursen, S.W. Hiebert, G. Grosveld, J.R. Downing, AML1, the target of multiple chromosomal translocations in human leukemia, is essential for normal fetal liver hematopoiesis, Cell 84 (1996) 321–330.
[12] M.J. Chen, T. Yokomizo, B.M. Zeigler, E. Dzierzak, N.A. Speck, Runx1 is required for the endothelial to haematopoietic cell transition but not thereafter, Nature 457 (2009) 887–891.
[13] Q. Wang, T. Stacy, M. Binder, M. Marin-Padilla, A.H. Sharpe, N.A. Speck, Disruption of the Cbfa2 gene causes necrosis and hemorrhaging in the central nervous system and blocks definitive hematopoiesis, Proc. Natl. Acad. Sci. U.S.A. 93 (1996) 3444–3449.
[14] M. Ichikawa, T. Asai, T. Saito, S. Seo, I. Yamazaki, T. Yamagata, et al., AML-1 is required for megakaryocytic maturation and lymphocytic differentiation, but not for maintenance of hematopoietic stem cells in adult hematopoiesis, Nat. Med. 10 (2004) 299–304.
[15] C.Q. Wang, V. Krishnan, L.S. Tay, D.W. Chin, C.P. Koh, J.Y. Chooi, et al., Disruption of Runx1 and Runx3 leads to bone marrow failure and leukemia predisposition due to transcriptional and DNA repair defects, Cell Rep. 8 (2014) 767–782.
[16] Y. Naoe, R. Setoguchi, K. Akiyama, S. Muroi, M. Kuroda, F. Hatam, et al., Repression of interleukin-4 in T helper type 1 cells by Runx/Cbf beta binding to the Il4 silencer, J. Exp. Med. 204 (2007) 1749–1755.
[17] Y.T. Hor, D.C. Voon, J.K. Koo, H. Wang, W.M. Lau, H. Ashktorab, et al., A role for RUNX3 in inflammation-induced expression of IL23A in gastric epithelial cells, Cell Rep. 8 (2014) 50–58.
[18] C.L. Langrish, Y. Chen, W.M. Blumenschein, J. Mattson, B. Basham, J.D. Sedgwick, et al., IL-23 drives a pathogenic T cell population that induces autoimmune inflammation, J. Exp. Med. 201 (2005) 233–240.
[19] J. Rennert, J.A. Coffman, A.R. Mushegian, A.J. Robertson, The evolution of Runx genes I. A comparative study of sequences from phylogenetically diverse model organisms, BMC Evol. Biol. 3 (2003) 4.
[20] S. Hughes, A. Woollard, RUNX in invertebrates, Adv. Exp. Med. Biol. 962 (2017) 3–18.
[21] A.J. Robertson, C.E. Dickey, J.J. McCarthy, J.A. Coffman, The expression of SpRunt during sea urchin embryogenesis, Mech. Dev. 117 (2002) 327–330.
[22] F. Yue, Z. Zhou, L. Wang, R. Sun, Q. Jiang, Q. Yi, et al., The essential roles of core binding factors CfRunt and CfCBFbeta in hemocyte production of scallop Chlamys farreri, Dev. Comp. Immunol. 44 (2014) 291–302.
[23] F. Yue, L. Wang, H. Wang, L. Song, Expression of hematopoietic transcription factors Runt, CBFbeta and GATA during ontogenesis of scallop Chlamys farreri, Dev. Comp. Immunol. 61 (2016) 88–96.
[24] R. Nimmo, A. Antebi, A. Woollard, mab-2 encodes RNT-1, a C. elegans Runx homologue essential for controlling cell proliferation in a stem cell-like developmental lineage, Development (Cambridge, England) 132 (2005) 5043–5054.
[25] J. Canon, U. Banerjee, Runt and Lozenge function in Drosophila development, Semin. Cell Dev. Biol. 11 (2000) 327–336.
[26] T. Braun, A. Woollard, RUNX factors in development: lessons from invertebrate model systems, Blood Cells Mol. Dis. 43 (2009) 43–48.
[27] J.A. Coffman, C.V. Kirchhamer, M.G. Harrington, E.H. Davidson, SpRunt-1, a new member of the runt domain family of transcription factors, is a positive regulator of the aboral ectoderm-specific CyIIIA gene in sea urchin embryos, Dev. Biol. 174 (1996) 43–54.
[28] T. Lebestky, T. Chang, V. Hartenstein, U. Banerjee, Specification of Drosophila hematopoietic lineage by conserved transcription factors, Science (New York, NY) 288 (2000) 146–149.
[29] L. Bataille, B. Auge, G. Ferjoux, M. Haenlin, L. Waltzer, Resolving embryonic blood cell fate choice in Drosophila: interplay of GCM and RUNX factors, Development (Cambridge, England) 132 (2005) 4635–4644.
[30] L. Canesi, G. Gallo, M. Gavioli, C. Pruzzo, Bacteria-hemocyte interactions and phagocytosis in marine bivalves, Microsc. Res. Tech. 57 (2002) 469–476.
[31] M. Jemaa, N. Morin, P. Cavelier, J. Cau, J.M. Strub, C. Delsert, Adult somatic progenitor cells and hematopoiesis in oysters, J. Exp. Biol. 217 (2014) 3067–3077.
[32] E.A. Dyrynda, R.K. Pipe, N.A. Ratcliffe, Sub-populations of haemocytes in the adult and developing marine mussel, Mytilus edulis, identified by use of monoclonal antibodies, Cell Tissue Res. 289 (1997) 527–536.
[33] Q. Xue, T. Renault, Monoclonal antibodies to European flat oyster Ostrea edulis hemocytes: characterization and tissue distribution of granulocytes in adult and developing animals, Dev. Comp. Immunol. 25 (2001) 187–194.
[34] J. Xing, X. Tang, Y. Ni, W. Zhan, Application of monoclonal antibody against granulocytes of scallop Chlamys farreri on granulocytes occurrence at different developmental stages and antigenic cross-reactivity of granulocytes in five other bivalve species, Fish Shellfish Immunol. 36 (2014) 315–319.
[35] X. Song, H. Wang, H. Chen, M. Sun, Z. Liang, L. Wang, et al., Conserved hemopoietic transcription factor Cg-SCL delineates hematopoiesis of Pacific oyster Crassostrea gigas, Fish Shellfish Immunol. 51 (2016) 180–188.
[36] X. Song, X. Xin, M. Dong, W. Wang, L. Wang, L. Song, The ancient role for GATA2/3 transcription factor homolog in the hemocyte production of oyster, Dev. Comp. Immunol. 82 (2018) 55–65.
[37] R. Liu, L. Qiu, Z. Yu, J. Zi, F. Yue, L. Wang, et al., Identification and characterisation of pathogenic Vibrio splendidus from Yesso scallop (Patinopecten yessoensis) cultured in a low temperature environment, J. Invertebr. Pathol. 114 (2013) 144–150.
[38] R. Beaz-Hidalgo, S. Balboa, J.L. Romalde, M.J. Figueras, Diversity and

pathogenecity of Vibrio species in cultured bivalve molluscs, Env. Microbiol. Rep. 2 (2010) 34–43.

[39] X. Song, X. Wang, L. Li, G. Zhang, Identification two novel nacrein-like proteins involved in the shell formation of the Pacific oyster Crassostrea gigas, Mol. Biol. Rep. 41 (2014) 4273–4278.

[40] T.A. Hall, BioEdit: a user-friendly biological sequence alignment editor and analysis program for Windows 95/98/NT, Nucleic Acids Symp. Ser. 41 (1999) 95–98.

[41] I. Letunic, P. Bork, 20 years of the SMART protein domain annotation resource, Nucleic Acids Res. 46 (2018) D493-d6.

[42] Ba AN. Nguyen, A. Pogoutse, N. Provart, A.M. Moses, NLStradamus: a simple Hidden Markov Model for nuclear localization signal prediction, BMC Bioinf. 10 (2009) 202.

[43] P.K. Smith, R.I. Krohn, G.T. Hermanson, A.K. Mallia, F.H. Gartner, M.D. Provenzano, et al., Measurement of protein using bicinchoninic acid, Anal. Biochem. 150 (1985) 76–85.

[44] S. Cheng, W. Zhan, J. Xing, X. Sheng, Development and characterization of monoclonal antibody to the lymphocystis disease virus of Japanese flounder Paralichthys olivaceus isolated from China, J. Virol. Methods 135 (2006) 173–180.

[45] V. Dyachuk, N. Odintsova, Development of the larval muscle system in the mussel Mytilus trossulus (Mollusca, Bivalvia), Dev. Growth Differ. 51 (2009) 69–79.

[46] R.M. Zucker, Whole insect and mammalian embryo imaging with confocal microscopy: morphology and apoptosis, Cytometry 69 (2006) 1143–1152.

[47] K.J. Livak, T.D. Schmittgen, Analysis of Relative Gene Expression Data Using Real-Time Quantitative PCR and the 2(-Delta Delta C(T)) Method, Methods (San Diego, Calif) vol. 25, (2001), pp. 402–408.

[48] M.M. Cohen Jr., Perspectives on RUNX genes: an update, Am. J. Med. Genet. A. 149a (2009) 2629–2646.

[49] Y. Li, X. Song, W. Wang, L. Wang, Q. Yi, S. Jiang, et al., The hematopoiesis in gill and its role in the immune response of Pacific oyster Crassostrea gigas against secondary challenge with Vibrio splendidus, Dev. Comp. Immunol. 71 (2017) 59–69.

[50] J.X. Ziniu Li, Tingting Lin, Wenbin Zhan, Localization and distribution of haemocytes in D larvae of scallop Chlamys farreri, Period Ocean Univ China Nat Sci Ed 40 (2010) 61–64.

[51] A.S. Mount, A.P. Wheeler, R.P. Paradkar, D. Snider, Hemocyte-mediated shell mineralization in the eastern oyster, Science (New York, NY) 304 (2004) 297–300.

[52] S. Li, Y. Liu, C. Liu, J. Huang, G. Zheng, L. Xie, et al., Hemocytes participate in calcium carbonate crystal formation, transportation and shell regeneration in the pearl oyster Pinctada fucata, Fish Shellfish Immunol. 51 (2016) 263–270.

[53] A. Zapata, B. Diez, T. Cejalvo, C. Gutierrez-de Frias, A. Cortes, Ontogeny of the immune system of fish, Fish Shellfish Immunol. 20 (2006) 126–136.

[54] Y.Y. Wan, GATA3: a master of many trades in immune regulation, Trends Immunol. 35 (2014) 233–242.

[55] N.K. Wilson, D. Miranda-Saavedra, S. Kinston, N. Bonadies, S.D. Foster, F. Calero-Nieto, et al., The transcriptional program controlled by the stem cell leukemia gene Scl/Tal1 during early embryonic hematopoietic development, Blood 113 (2009) 5456–5465.

[56] W.T. Nottingham, A. Jarratt, M. Burgess, C.L. Speck, J.F. Cheng, S. Prabhakar, et al., Runx1-mediated hematopoietic stem-cell emergence is controlled by a Gata/Ets/SCL-regulated enhancer, Blood 110 (2007) 4188–4197.

[57] M.R. Tijssen, A. Cvejic, A. Joshi, R.L. Hannah, R. Ferreira, A. Forrai, et al., Genome-wide analysis of simultaneous GATA1/2, RUNX1, FLI1, and SCL binding in megakaryocytes identifies hematopoietic regulators, Dev. Cell 20 (2011) 597–609.